Segmentation Method for Manipulation Task Based on Measurement of Force Imposed by a Human Hand on an Object

Kazuya Matsuo*, Kouji Murakami*, Tsutomu Hasegawa*, Kenji Tahara*, and Ryo Kurazume*
*Information Science and Electrical Engineering, Kyushu University, Fukuoka, JAPAN

***Abstract*— This paper proposes a segmentation method of human manipulation task based on measurement of contact force imposed by a human hand on a grasped object. We define an index measure for segmenting a human manipulation task into primitives. The indices are calculated from the set of the contact forces measured at all the contact points during a manipulation task. Then, we apply the EM algorithm to the set of the indices in order to segment the manipulation task into primitives. These primitives are mapped onto the robotic hand to impose appropriate contact forces on a grasped object. In the experiments, manipulation tasks performed in daily human life have been successfully segmented.**

I. Introduction

A multi-jointed multi-fingered robotic hand is a potentially dexterous hand like a human hand [1]. However, it is very difficult for us to manually and directly write a motion program of multiple fingers moving synchronously and cooperatively to execute a task. Programming-by-demonstration [2][3] is often used in order to overcome this difficulty. In the programming-by-demonstration, a motion program for the robotic hand is generated based on the motion data of actual tasks executed by a human.

Direct mapping of joint angle trajectories of the human hand onto the robotic hand has been reported [4] for programming-by-demonstration. However, the direct mapping can not be applied to the robotic hand whose configuration is different from that of the human hand. Another method is mapping of positions of human fingertips onto the robotic hand [5]. This method generates joint angle trajectories of the robotic hand from the positions of the human fingertips by solving inverse kinematics of the robotic hand. This method may easily fail in keeping stable grasp of an object because it does not assure stable grasping force. Contact information between the palm and the grasped object is not mapped onto the robotic hand by this position mapping.

In order to overcome these problems, higher level mapping of symbolized manipulation primitives onto the robotic hand has been proposed. This method recognizes a task from the motion data of the human hand: continuous human hand motion is segmented, and symbolized according to the meaning of a particular motion in the context of the task. Each symbol represents a particular manipulation primitive. The task is represented as a sequence of symbols. The robotic hand will therefore be able to autonomously perform various tasks by executing a sequence of corresponding manipulation primitives if the symbols representing manipulation primitives are recognized. Bernardin *et al.* [6] presented a method to recognize continuously executed sequences of grasping gestures.

Particular shapes of grasps by the human hand are usually used as keys to recognize manipulation primitives in related work on human motion recognition [6][7][8][9][10]. Classified particular shapes of the human hand are called grasp types. Cutkosky proposed a grasp taxonomy [11] consisting of 16 hand shapes used by humans working with tools and metal parts. Kamakura, an occupational therapist, proposed a grasp taxonomy [12] consisting of 14 hand shapes used in daily life. These grasp taxonomies are classified based on observations of particular shapes of the human hand.

However, the grasp types do not contain force information imposed on the object grasped by the human hand. So, the robotic hand may not impose the appropriate force on the grasped object when a mapping of shape-based grasp type is applied. Required force information consists of magnitude and direction of the forces at the contact points. The force information imposed by the human hand is an important property to be mapped onto the robotic hand in the programming-by-demonstration. The robotic hand imposes the appropriate force on the grasped object when a mapping of force-based primitive is applied.

This paper proposes a segmentation method of human manipulation task based on contact force imposed on an object grasped by a human hand. The remainder of the paper is organized as follows. Section Ⅱ explains the segmentation method of manipulation task based on force measurement at the contact points. The designed device to measure forces imposed by a human hand is described in Section Ⅲ. Section I V describes the experiments for segmenting human motion of a screw manipulation task and a writing task. The conclusions of the present study and the future work are presented in Section V.

II. Segmentation Method of Manipulation Task

We propose a segmentation method of human manipulation task. First, we measure contact force imposed on an object grasped by a human hand during a manipulation task. Then, we define an index measure for segmenting the manipulation

task. The index is calculated from the set of the contact forces at all the contact points. We call the index *contact force index*. We assume that a human manipulation task is composed of primitives: each of them is characterized by particular distribution pattern of force and torque at contacts on the object with the hand so that the appropriate interaction and constraint are generated to satisfy the task requirements. The time series data of contact force are segmented to be primitives by applying a cluster analysis to the set of *the contact force indices*.

A. Analyzing grasping force of a human hand on an object

A human worker adjusts the magnitude and direction of contact force when he grasps an object so that suitable constraints and external force are generated to perform the particular task. Different force is required for the same object if the task context is different. For example, the grasping force of a hammer when the worker carries it is different from the force required when he hits a nail with the hammer even though the grasping shape of the hand is similar. Strategy to adjust the grasping force may be acquired through experience and learning of the worker. It would be possible to recognize the task primitive by analyzing the time series of grasping force even though the grasping shape of the hand does not change.

It is very difficult to map all the forces of a human hand imposed at all the contact points onto a robotic hand. Thus, we calculate *the contact force index* to evaluate and recognize the requirements of grasp which in turn leads to segment the manipulation task into primitives. Then, the primitives are mapped to the actual robotic hand.

B. Contact force index

Many works have been reported on the contact force imposed on an object grasped by a robotic hand. Force closure [13] is often used to characterize the grasp stability. The force closure means any wrench can be expressed by a positive combination of contact point wrenches. A robotic hand performing the force closure can influence the object such that any external disturbance can be nullified. Grasp quality [14] is an index for evaluating the stability of a grasp. Miller and Allen computed the grasp quality from a shape of a wrench space. These are indices for evaluating the stability of a grasp performed by a robotic hand. Thus, these are not suitable for an index for extracting primitives from a manipulation task performed by a human hand.

We propose *the contact force index*: an index for extracting primitives from a manipulation task performed by a human hand. *The contact force index* is calculated from the shapes of two convex hulls formed by the contact forces and the torques at all the contact points. *The contact force index* is suitable for mapping onto a robotic hand because the mapping using *the contact force index* does not constrain the numbers and the positions of contact points on the object. So, a robotic hand is able to apply the precision grasp to this mapping. We formulate a method for calculating *the contact force index* on the assumptions as follows:

1) A contact between a human hand and a grasped object is the point contact with friction.
2) The normal direction of a contact force at each contact point depends upon the contacting surface of the object.
3) The grasping force applied to the object by the human hand is composed of the contact forces at all the contact points.

We explain the formalization to calculate *the contact force index*. Firstly, we construct two matrices: $\boldsymbol{W_f}$ is the matrix consisting of the contact force vectors at all the contact points and $\boldsymbol{W_t}$ is the matrix consisting of the torque vectors at all the contact points. Two matrices are expressed as:

$$\boldsymbol{W_f} = \begin{pmatrix} \boldsymbol{f_1} & \boldsymbol{f_2} & \cdots & \boldsymbol{f_N} \end{pmatrix} \in \Re^{3\times N}, \tag{1}$$

$$\boldsymbol{t_i} = \boldsymbol{p_i} \times \boldsymbol{f_i} \quad (1 \le i \le N), \tag{2}$$

$$\boldsymbol{W_t} = \begin{pmatrix} \lambda\boldsymbol{t_1} & \lambda\boldsymbol{t_2} & \cdots & \lambda\boldsymbol{t_N} \end{pmatrix} \in \Re^{3\times N}, \tag{3}$$

where $\boldsymbol{f_i}$ is the contact force vector at the i th contact point, $\boldsymbol{t_i}$ is the torque vector at the i th contact point, $\boldsymbol{p_i}$ is the position vector of the i th contact point, λ is a torque multiplier that relates units of torque to units of force, and N is the number of contact points (Fig. 1). $\boldsymbol{f_i}$ and $\boldsymbol{p_i}$ are expressed with respect to a same coordinate system. We have enforced $|\lambda\boldsymbol{t_i}| \le |\boldsymbol{f_i}|$ by choosing $\lambda = \frac{1}{r}$, where r is the maximum distance of the contact points from the torque origin. This will ensure that *the contact force index* is independent of object scale.

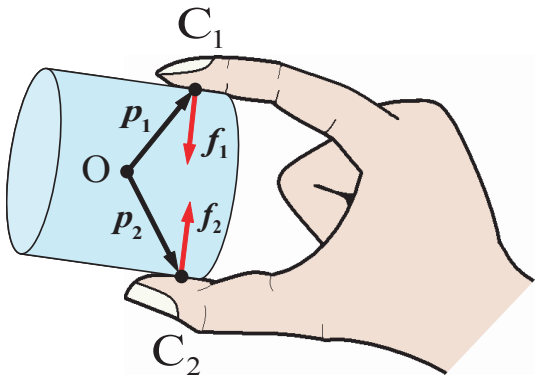

Fig. 1. Defined vectors to calculate *the contact index*: $\boldsymbol{f_i}$ is the contact force vector at the i th contact point, $\boldsymbol{p_i}$ is the position vector of the i th contact point, and C_i is the i th contact point ($i = 1, 2$).

Secondly, we calculate the singular values of $\boldsymbol{W_f}$ and $\boldsymbol{W_t}$ in order to investigate the shapes of two convex hulls formed by the total $\boldsymbol{f_i}$ and the total $\boldsymbol{t_i}$ respectively. The singular values of $\boldsymbol{W_f}$ and $\boldsymbol{W_t}$ represent the axes of ellipsoids which approximate the two convex hulls respectively. The singular values of $\boldsymbol{W_f}$ and $\boldsymbol{W_t}$ are calculated as follows:

$$\boldsymbol{W_f} = \boldsymbol{U_f}\boldsymbol{\Sigma_f}\boldsymbol{V_f^T}, \tag{4}$$

$$\boldsymbol{\Sigma_f} = diag(\sigma_{f1}, \sigma_{f2}, \sigma_{f3}) \quad (\sigma_{f1} \ge \sigma_{f2} \ge \sigma_{f3} \ge 0), \tag{5}$$

$$\boldsymbol{W_t} = \boldsymbol{U_t}\boldsymbol{\Sigma_t}\boldsymbol{V_t^T}, \tag{6}$$

$$\boldsymbol{\Sigma_t} = diag(\sigma_{t1}, \sigma_{t2}, \sigma_{t3}) \quad (\sigma_{t1} \ge \sigma_{t2} \ge \sigma_{t3} \ge 0), \tag{7}$$

where σ_j $(j = f1, f2, f3, t1, t2, t3)$ are the singular values, $\boldsymbol{U_k}$ $(k = f, t)$ are 3-by-3 orthogonal matrices, and $\boldsymbol{V_k}$ are N-by-N orthogonal matrices.

Lastly, *the contact force index* (***CFI***) is composed of the calculated 6 singular values.

$$\boldsymbol{CFI} = \begin{pmatrix} \sigma_{f1} & \sigma_{f2} & \sigma_{f3} & \sigma_{t1} & \sigma_{t2} & \sigma_{t3} \end{pmatrix}. \quad (8)$$

If manipulation primitives segmented by using *the contact force index* are mapped onto a robotic hand, we can decide the appropriate contact force imposed by the robotic hand. The magnitude of the appropriate contact force is decided based on the singular values. The direction of the appropriate contact force is decided based on $\boldsymbol{U_f}$, $\boldsymbol{V_f}$, $\boldsymbol{U_t}$, and $\boldsymbol{V_t}$.

C. Segmentation of manipulation task into primitives by applying a cluster analysis

We apply a cluster analysis to the set of *the contact force indices* in order to segment a manipulation task into primitives (Fig. 2). We employ the expectation-maximization (EM) algorithm [15] for this cluster analysis. The EM algorithm segments data into the specified number of clusters under the assumption that each cluster shows a normal distribution. Each *contact force index* calculated from contact forces includes the force measurement error. We suppose that the distribution of the force measurement error is the normal distribution. Thus, we use the EM algorithm.

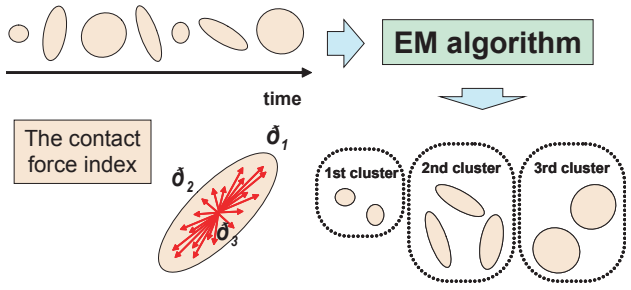

Fig. 2. Cluster analysis to the set of *the contact force indices* for segmentation of manipulation task into primitives.

Each of clusters segmented by the EM algorithm is treated as a manipulation primitive. We arbitrarily select the number of the extracted primitives by choosing the specified number of the clusters.

III. Device for Measuring Contact Force

To implement our method, we need to measure contact force imposed by a human hand on a grasped object. One direct way would be to attach pressure sensors on the contacting surface of the human hand. Discreet miniature pressure sensors are still too large and thick to attach to the human hand surface. It would obstruct natural motion of human hand during object manipulation. Thin film-type pressure sensor easily deforms itself according to the finger motion if it is attached to the finger surface, thus it outputs erroneous contact pressure. In addition, joint angles of fingers must be measured to obtain contact force direction with respect to the 3D task coordinate system. Joint angle measurement of human hand is difficult. Error of joint angle measurement badly affects the performance of our method.

We attach the pressure sensors onto the surface of the object to be manipulated. We have developed sensing device as shown in Fig. 3. Total of 60 pressure sensors (Flexi Force, Nitta Corp.) are attached to the surface of the device. The device is composed of a brass 6-sided regular prism and a wooden cone on its top. Ten pressure sensors are installed on each side face of the 6-sided prism. The mass of the device is 253[g].

The size of the device and the placement of the installed 60 pressure sensors are shown in Fig. 4. The orange circles in Fig. 4 indicate pressure sensors distributed on the device.

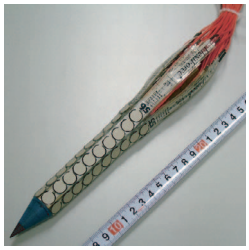

Fig. 3. Photograph of the contact force sensing device.

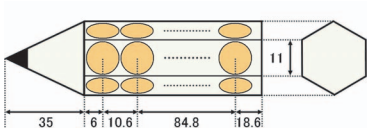

Fig. 4. Size of the contact force sensing device and placement of the 60 pressure sensors.

A photograph of the sensing part of the pressure sensor is shown in Fig. 5. The sensing part has a circular shape whose diameter is 9.5[mm], and the thickness of the sensing part is 0.2[mm]. The specifications of the pressure sensor are shown in TABLE I. The pressure sensor measures normal forces to itself.

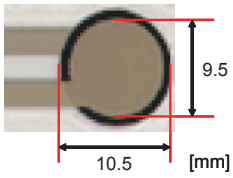

Fig. 5. Photograph of the sensing part of the pressure sensor.

TABLE I
Specifications of the Pressure Sensor

Maximum capacity	110[N]
Resistance under no-load	10[MΩ]
Resistance under maximum-load	20[kΩ] ± 15%
Hysteresis	< 4.5%
Linearity	< ± 5%

The contact force is decomposed into the normal force and the tangential force. Commercially available thin film sensor measures the normal force only. So, we investigate the results of our method in the case of measuring only the normal force in this report. To analyze the influence of the tangential components is future work.

IV. Experiments

We applied our method to two different manipulation tasks performed in daily human life: a screw manipulation task and

a writing task. A human subject performed the manipulation tasks with the contact force sensing device. The subject was male of age 25 years.

A. Screw manipulation task

The subject rotated the contact force sensing device like a screwdriver. The screw manipulation task is executed in the order explained as follows:

1) Noncontact between the device and a hand (Fig. 6-a).
2) Rotating the device clockwise (Fig. 6-b).
3) Noncontact between the device and the hand.
4) Repeat 2) and 3) twice.
5) Rotating the device counterclockwise (Fig. 6-c).
6) Noncontact between the device and the hand.
7) Repeat 5) and 6) twice.

He touches different parts of the device when he regrasps it in the step 2) and 5). The influence of the wiring of the device on sensor reading is negligible during this manipulation task.

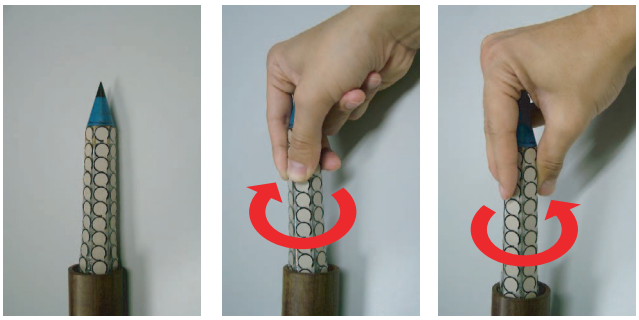

a: noncontact b: clockwise c: counterclockwise

Fig. 6. Snapshots of the screw manipulation task.

We applied our method to the screw manipulation task. Sampling rate of the contact force sensing device is 33[Hz]. In the implementation of the method, the parameters are determined as follows: the coordinate system of the contact force sensing device is defined as shown in Fig. 7. The magnitude and the direction of the contact force vector $\boldsymbol{f_i}$ is obtained from the output and the position of the i th sensor. A position vector $\boldsymbol{p_i}$ is decided from the center position of the sensing part of the i th sensor and the origin of the coordinate system. The value of r is approximately 95.9[mm]: the maximum distance of the sensors from the origin.

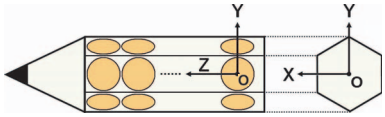

Fig. 7. Coordinate system of the sensing device.

1) Comparison between primitives extracted by the method and segmentations of human motion by human intuition: We applied our method to the screw manipulation task in order to segment the task into 2 primitives. The result is shown in Fig. 8.

Horizontal axis shows the elapsed time. Vertical axis shows the extracted primitives as the clusters. The colors of the data

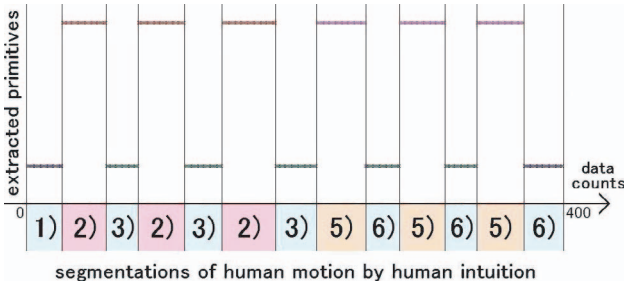

Fig. 8. Segmented the screw manipulation task into 2 primitives. 1), 3), and 6) are segmentations labeled by 'noncontact'. 2) is a segmentation labeled by 'clockwise'. 5) is a segmentation labeled by 'counterclockwise'. Sampling rate of data count is 33[Hz].

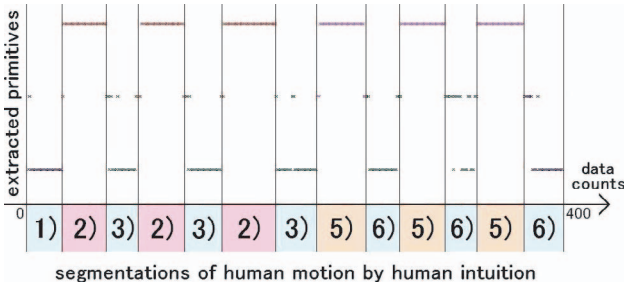

Fig. 9. Segmented the screw manipulation task into 3 primitives.

and the division by the vertical lines indicate 3 groups classified through visual observation by human intuition: 'noncontact', 'clockwise', and 'counterclockwise'. These groups are classified independently of the primitives extracted by our method. The 2 primitives (Fig. 8) are interpreted as 'noncontact' and 'rotation (clockwise & counterclockwise)'. The 2 primitives are similar to segmentations of human motion by human intuition.

2) Selection of the number of the primitives by choosing the number of the clusters: We also applied our method to the screw manipulation task in order to segment the task into 3 primitives. The result is shown in Fig. 9. The 3 primitives (Fig. 9) are interpreted as 'noncontact', 'rotation (clockwise & counterclockwise)', and 'approach or release'. 'approach or release' means the transitions between 2 segmentations labeled by 'noncontact' and 'rotation'.

3) Advantage of contact force index against raw sensor output: We segmented the screw manipulation task into 2 primitives by applying the EM algorithm to the set of the raw sensor outputs: the 60 dimensional data provided from the 60 pressure sensors of the device. The segmentation result is shown in Fig. 10.

The extracted 2 primitives by using the 6 dimensional *contact force indices* (Fig. 8) are more similar to the groups classified by human intuition than those by using the raw sensor outputs (Fig. 10). Rotation of the device is a cause of this result. For the convenience of comprehension, we discuss a case of only the 6 pressure sensors. We explain two grasping situations: they are different in the contact points (Fig. 11-(a) and Fig. 11-(b)). The numerals in Fig. 11 indicate the serial numbers of the 6 pressure sensors. Every force imposed at the contact points is the same magnitude 'F'. A sensor output is expressed as a

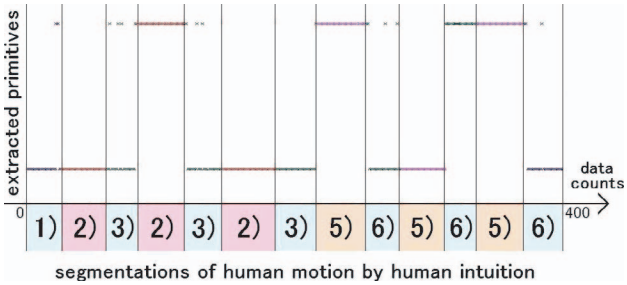

Fig. 10. Segmented the screw manipulation task into 2 primitives by using the 60 dimensional data provided from the contact force sensing device.

vector consisting of outputs of the 6 pressure sensors. Thus, the sensor output in Fig. 11-(a) is $\boldsymbol{F_a}$ = (F 0 F 0 F 0), and the sensor output in Fig. 11-(b) is $\boldsymbol{F_b}$ = (0 F 0 F 0 F). In addition, the sensor output in the case of 'noncontact' is $\boldsymbol{F_o}$ = (0 0 0 0 0 0).

The Euclidean distances between $\boldsymbol{F_a}$, $\boldsymbol{F_b}$, and $\boldsymbol{F_o}$ are calculated as follows:

$$|\boldsymbol{F_a} - \boldsymbol{F_b}| = 6F, \tag{9}$$

$$|\boldsymbol{F_a} - \boldsymbol{F_o}| = |\boldsymbol{F_b} - \boldsymbol{F_o}| = 3F, \tag{10}$$

$$\therefore |\boldsymbol{F_a} - \boldsymbol{F_b}| > |\boldsymbol{F_a} - \boldsymbol{F_o}| = |\boldsymbol{F_b} - \boldsymbol{F_o}|. \tag{11}$$

The Euclidean distance between the two grasping situations ($\boldsymbol{F_a}$ and $\boldsymbol{F_b}$) is greater than that between 'noncontact' ($\boldsymbol{F_o}$) and each grasping situation (see Eq. (11)). Therefore, the two grasping situations are extracted as different primitives in the case of using the raw sensor outputs. In contrast, *the contact force indices* of $\boldsymbol{F_a}$ and $\boldsymbol{F_b}$ are of equal magnitude. Therefore, the two grasping situations are extracted as the same primitive in the case of using *the contact force indices*.

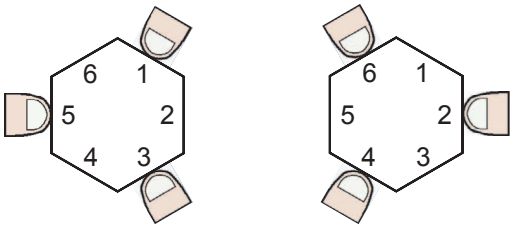

Fig. 11. Two grasping situations which are different in the contact points.

B. Writing task

The subject drew lines with the contact force sensing device. The sequence of writing task is as follows:

1: The device is on a desk (Fig. 12-a).
2: Taking up the device.
3: Carrying the device above paper (Fig. 12-b).
4: Changing a grasping form for writing (Fig. 12-c).
5: Grasping the device for writing (Fig. 12-d).
6: Drawing a vertical line.
7: Moving the tip of the device.
8: Drawing a vertical line.
9: Moving the tip of the device.
10: Drawing a horizontal line.
11: Moving the tip of the device.
12: Drawing a horizontal line.
13: Grasping the device for writing.
14: Carrying the device back where it was (Fig. 12-e).
15: Changing a grasping form and putting the device on the desk (Fig. 12-f).
16: The device is on the desk without a touch.

We classified the 16 segmentations mentioned above into 8 groups by human intuition.

I: The device is on the desk without a touch (1, 16).
II: Taking up the device (2).
III: Carrying the device (3, 14).
IV: Changing a grasping form (4, 15).
V: Grasping the device for writing (5, 13).
VI: Drawing a vertical line (6, 8).
VII: Drawing a horizontal line (10, 12).
VIII: Moving the tip of the device (7, 9, 11).

We segmented the writing task into 8 primitives in the same way described in Section IV-A. The segmentation result is shown in Fig. 13. We successfully segmented the writing task into the 8 primitives which are similar to the 8 groups classified by human intuition.

V. Conclusions and Future Work

A. Conclusions

We defined *the contact force index* for segmenting human manipulation task into primitives. *The contact force index* was calculated from the set of the contact forces at all the contact points. Then, we proposed a segmentation method of human manipulation task into primitives by applying the EM algorithm to the set of *the contact force indices*. In the experiments, we applied our method to manipulation tasks performed in daily human life: a screw manipulation task and a writing task. The results of the experiments are summarized as follows:

1) We successfully segment the tasks into primitives which are similar to segmentations of human motion by human intuition.
2) The primitives are extracted regardless of the relative position/orientation between a human hand and an object during the manipulation tasks.

B. Future work

We will segment various manipulation tasks performed in daily human life into primitives. In addition, we will map the primitives onto robotic hands in the programming-by-demonstration.

References

[1] A. Bicchi, Hands for Dexterous Manipulation and Robust Grasping: A Difficult Road Toward Simplicity, *IEEE Trans. on Robotics and Automation*, Vol. 16, No. 6, 2000, pp. 652–662.
[2] K. Ikeuchi and T. Suehiro, Toward an Assembly Plan from Observation Part I: Task Recognition With Polyhedral Objects, *IEEE Trans. on Robotics and Automation*, Vol. 10, No. 3, 1994, pp. 368–385.

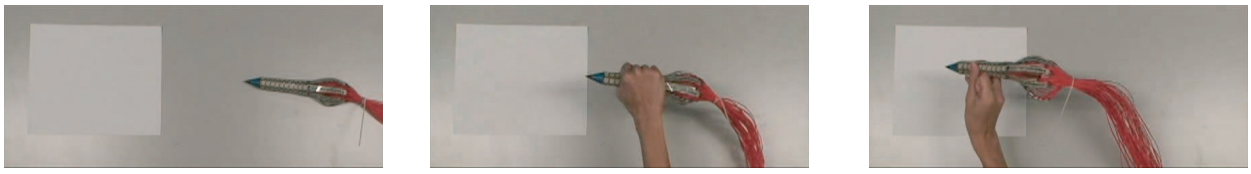

a: The device is on the desk.

b: Carrying the device above paper.

c: Changing a grasping form for writing.

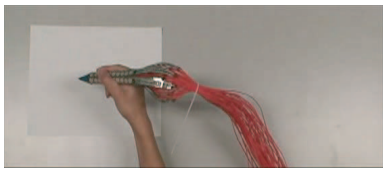

d: Grasping the device for writing.

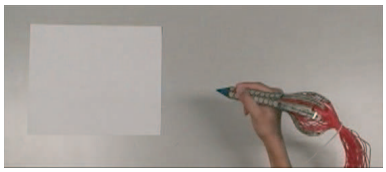

e: Carrying the device back where it was.

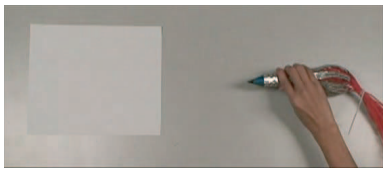

f: Changing a grasping form and putting the device on the desk.

Fig. 12. Snapshots of the writing task.

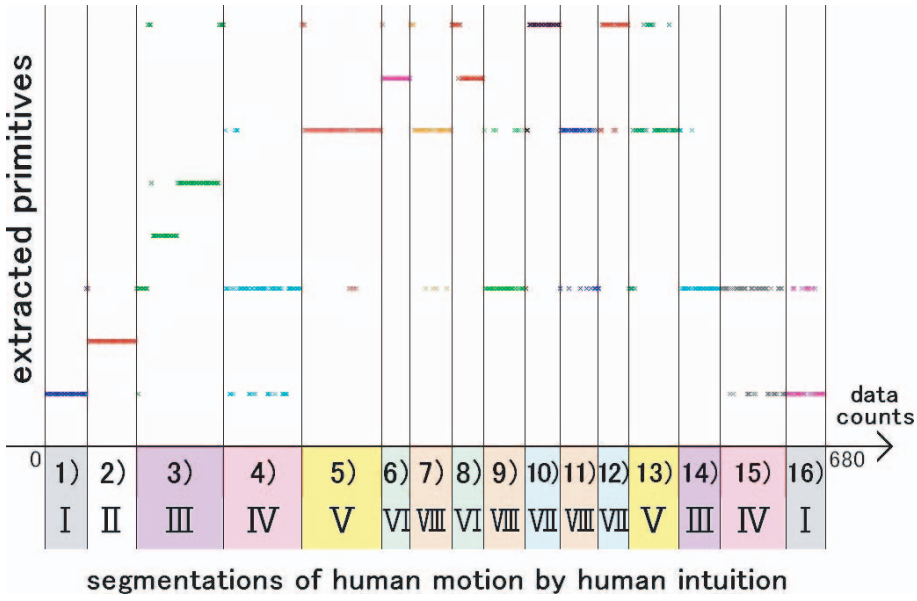

Fig. 13. Segmented the writing task into 8 primitives.

[3] Y. Kuniyoshi, M. Inaba, and H. Inoue, Learning by Watching: Extracting Reusable Task Knowledge from Visual Observation of Human Performance, *IEEE Trans. on Robotics and Automation*, Vol. 10, No. 6, 1994, pp. 799–822.

[4] K. J. Kyriakopoulos, J. Van Riper, A. Zink, and H. E. Stephanou, Kinematic analysis and position/force control of the Anthrobot dexterous hand, *IEEE Trans. on Systems, Man, and Cybernetics, Part B*, Vol. 27, No. 1, 1997, pp. 95–104.

[5] J. Hong and X. Tan, "Calibrating a VPL DataGlove for teleoperating the Utah/MIT hand", *Proc. of the 1989 IEEE Int'l Conf. on Robotics and Automation*, 1989, pp. 1752–1757.

[6] K. Bernardin, K. Ogawara, K. Ikeuchi, and R. Dillmann, A Sensor Fusion Approach for Recognizing Continuous Human Grasping Sequences Using Hidden Markov Models, *IEEE Trans. on Robotics*, 2005, Vol. 21, No. 1, pp. 47–57.

[7] J. Aleotti and S. Caselli, "Grasp Recognition in Virtual Reality for Robot Pregrasp Planning by Demonstration", *Proc. of the 2006 IEEE Int'l Conf. on Robotics and Automation*, 2006, pp. 2801–2806.

[8] L. Y. Chang, N. S. Pollard, T. M. Mitchell, and E. P. Xing, "Feature selection for grasp recognition from optical markers", *Proc. of the 2007 IEEE/RSJ Int'l Conf. on Intelligent Robots and Systems*, 2007, pp. 2944–2950.

[9] S. Ekvall and D. Kragic, "Grasp Recognition for Programming by Demonstration", *Proc. of the 2005 IEEE Int'l Conf. on Robotics and Automation*, 2005, pp. 760–765.

[10] M. Kondo, J. Ueda, Y. Matsumoto, and T. Ogasawara, "Perception of Human Manipulation Based on Contact State Transition", *Proc. of the 2004 IEEE/RSJ Int'l Conf. on Intelligent Robots and Systems*, 2004, pp. 100–105.

[11] M. R. Cutkosky, On Grasp Choice, Grasp Models, and the Design of Hands for Manufacturing Tasks, *IEEE Trans. on Robotics and Automation*, 1989, Vol. 5, No. 3, pp. 269–279.

[12] N. Kamakura, M. Matsuo, H. Ishii, F. Mitsuboshi, and Y. Miura, Patterns of static prehension in normal hands, *The American J. of Occupational Therapy*, 1980, Vol. 34, No. 7, pp. 437–445.

[13] J. K. Salisbury and B. Roth, Kinematic and Force Analysis of Articulated Hands, *ASME J. of Mechanisms, Transmissions, and Automation in Design*, 1982, Vol. 105, pp. 33–41.

[14] A. T. Miller and P. K. Allen, "Examples of 3D Grasp Quality Computations", *Proc. of the 1999 IEEE Int'l Conf. on Robotics and Automation*, 1999, pp. 1240–1246.

[15] A. P. Dempster, N. M. Laird, and D. B. Rubin, Maximum Likelihood from Incomplete Data via the EM Algorithm, *J. of the Royal Statistical Society, Series B (Methodological)*, 1977, Vol. 39, No. 1, pp. 1–38.